Xin et al.

Supplementary Information Text

SI Materials and Method

Purification of recombinant proteins

Pyrogen-free reagents were employed. Prior to use, columns and equipment (Akta Explorer System) were sanitized by exposure to 0.5 N NaOH. Conditioned media from transfected cells were adjusted to PBS, 0.01% polysorbate (PS) 20. PS20 was added to buffers at all steps. After centrifugation at 20,000 g for 30 minutes, supernatants were subjected to protein A (PA) affinity chromatography using a Hi-Trap MabSelect SuRe (5 ml, GE Healthcare). After loading, the column was washed with 20 mM ethanolamine, pH 9.2, 1.2 M NaCl, prior to elution with 0.1 M citric acid, pH 3.0, which was immediately neutralized. The PA elution pool was then diluted in 20 mM ethanolamine, pH 9.2, and applied to Hi-Trap Q (GE Healthcare) anion-exchange column. The bound material was eluted with a gradient of NaCl. The flow-through, which contained the purified recombinant protein, was immediately adjusted to 20 mM Tris, pH 6.8, and then concentrated through binding to heparin-sepharose (Hi Trap™ Heparin HP). After a wash with 0.2-0.45 M NaCl (depending on the construct), the chimeric VEGFR1 protein was eluted with 1 M NaCl. The final polishing step consisted of size-exclusion chromatography (SEC). Finally, the proteins were buffer-exchanged by dialysis into 10 mM Tris, pH 6.8, 10 mM histidine, 5% trehalose, 40 mM NaCl, 0.01% PS20. To determine endotoxin levels, ToxinSensor Chromogenic LAL Endotoxin Assay Kit (GenScript, L00350) was used according to the manufacturer's protocol.

Promega VEGF bioassay

In addition to assays with primary BCEC, which last 5-6 days, we used a recently developed rapid VEGF Bioassay kit (GA2001, Promega). This bioluminescent cell-based assay measures VEGF stimulation using luciferase as a readout in order to measure effect of inhibitors on VEGF-induced signal transduction. In brief, 25 μl of KDR/NFAT-RE HEK293 cells engineered to express KDR and the NFAT response element (RE) upstream of Luc2P, were seeded into 96-well plate. 25 μl of assay buffer with serial diluted V1233, V233, Eylea® or human IgG1 (BE0297, BioXcell) were added as indicated, then an additional 25 μl of assay buffer with $VEGF_{165}$ was added to each well and incubated at 37°C in a humidified atmosphere with 5% CO_2. The final concentration of $VEGF_{165}$ was 20 ng/ml. After a 6-hour incubation, 75 μl Bio-Glo™ 80 Reagent was added, and luminescence was quantified using SpectraMax M5 microplate reader. Data were fitted to a 4PLx®curve using GraphPad Prism® software. The experiment was repeated three times.

***In vitro* binding to bovine vitreous**

Bovine vitreous samples (InVision BioResource, Seattle, WA) were thawed at 4°C and then diluted 1:1 with PBS, filtered through 0.22 μm filter, aliquoted and stored at -80° C. Total protein concentrations were measured by the Pierce BCA protein assay. Costar 96-well EIA/RIA stripwells were coated with vitreous (1 μg/well) for 4hr at RT, followed by one wash with PBS-0.1% Tween 20 (PBS-T). To each well, 0.08 to 10 nM chimeric VEGF receptor protein was added in a 50 μl volume and incubated overnight at 4°C. Plates were be then washed with PBS-T, and

incubated with AP-conjugated goat anti-human Fc (1:2000, Invitrogen, #A18832) for 1hr at RT. Plates were washed with PBS-T before 1 step PNPP substrate (Thermo Scientific, Rockford, IL, #37621) for 15-30 min at RT. Absorbance will be measured at 405 nm.

Laser-induced choroidal neovascularization (CNV) model

Male C57BL/6J mice (6-8 week) were anesthetized with ketamine/Xylazine cocktail before laser treatment. CNV lesions were induced by laser photocoagulation using a diode laser (IRIDEX, Oculight GL) and a slit lamp (Zeiss) with a spot size of 50 μm, power of 180 mW and exposure duration of 100 ms. (1, 2). Four laser burns were typically induced at 3, 6, 9 and 12 o'clock position around the optic disc in each eye. Different constructs or IgG isotype control were injected intravitreally, at the dose of 2.5 μg per eye, in a 1µl volume. Eylea® was used as a positive control at 2.5 or 25 μg. One day after injection, laser treatment was conducted and eyes were enucleated and fixed in 4% paraformaldehyde (PFA) for 15 min, 7 days after laser treatment. In a separate set of studies, selected constructs were injected once 1 day, 7 days or 14 days prior to laser treatment. Choroid-sclera complexes and retinas were separated and anti-CD31 immunofluorescence (IF) was performed to evidence the vasculature by whole mount staining of both retina and choroidal tissues. For CD31 IF, rat anti-mouse antibody BD 550274 was diluted 1:100 and incubated overnight at 4^{o}C. After 4-hour incubation with a secondary anti-rat antibody (Life Technologies A11006), whole mounts were imaged at 488 nm. Quantification of neovascularization in lesion area and vascular density in retina was carried out by Image J. P values were assessed by Student's t test (significant change, $p<0.05$).

Oxygen-induced retinopathy model

The Oxygen Induced Retinopathy (OIR) mouse model is a well-established method that has proven useful in delineating the molecular changes in ischemic vascular eye disease (3, 4). Using an enclosed chamber, neonatal mice are exposed to 75% oxygen from postnatal day 7 (P7) until P12, and then returned to 21% oxygen (room air). This exposure to hyperoxia causes vessel regression in the central retina and the cessation of normal radial vessel growth, mimicking the vaso-obliterative phase of ischemic vasculopathies. Upon return to room air, the avascular areas of retina become hypoxic (5, 6). This hypoxia induces the expression of angiogenic factors, especially VEGF(7), resulting in the growth of aberrant retinal neovascularization at the junctions of vascular and avascular retina. To test the effects of inhibitors, intravitreal injections were performed prior to exposure to hyperoxia. Wild-type C57BL/6j mice at P7 were anesthetized using isoflurane flowing through a rodent facemask. The eyelids were opened using a Vannas microdissection scissors and pulled back to expose the eye. Next, 0.5 µl of solution was injected using a custom 34-gauge Hamilton syringe into the vitreous cavity. The needle was left in the eye for 30 seconds after injection and withdrawn slowly to minimize leakage. This procedure was repeated in the fellow eye with injection of equimolar human IgG1 as control (Bio X Cell, West Labanon, NH). Eylea®, various constructs were tested versus control IgG1 at a concentration of 3.25 µg (molar equivalent with Eylea 2.5 µg and V1233 3.8 µg). The eyelids were covered with antibiotic ointment. Litters were then be placed in a 75% hyperoxic chamber from P7-P12 to generate the OIR phenotype. A minimum of 3 separate litters (5-10 pups each) were used for experiments at each of P12 and P17. At these timepoints, the animals were sacrificed, and the eyes enucleated, dissected, and the vessels stained with BSL-FITC. The retinas were flat-mounted

and imaged by fluorescent microscopy. Vaso-obliteration and neovascularization were analyzed using automated software, as described (8).

Supplementary Figure Legends

Fig. S1

Inhibitory effects of fusion protein on BCEC proliferation stimulated by $VEGF_{165}$ or $VEGF_{121}$. Results are expressed as % of inhibition of VEGF-stimulated proliferation relative to control. Cell numbers were determined by relative fluorescence unit (RFU) 530/590 (Excitation/Emission), average of triplicates.

Fig S2

Inhibitory effects of recombinant VEGF receptor Fc-fusion proteins on HUVEC proliferation. V123, V1233, V233, V23 or Eylea® (10-2000 ng/ml) was added along with $VEGF_{165}$ (10 ng/ml) for 3 days, and cell viability was determined. Results are expressed as % of inhibition of VEGF-stimulated proliferation relative to control. Cell numbers were determined by relative fluorescence unit (RFU) 530/590 (Excitation/Emission), average of triplicates.

Fig. S3

The Promega VEGF Bioassay was used to measure the inhibitory activity of V1233, V233, Eylea® or control IgG. KDR/NFAT-RE HEK293 cells were incubated with serial dilutions of the above proteins in the presence of 20 ng/ml of $VEGF_{165}$. After a 6-hour incubation, Bio-Glo™ 80 Reagent was added, and luminescence was quantified using SpectraMax M5 microplate reader. Data were fitted to a 4PLx®curve using GraphPad Prism® software

Fig. S4

Crystal structure of VEGF/VEGFR2 complex (3V2A) was superimposed on the crystal structure of the VEGF/VEGFR1 complex (5T89). VEGFR1 residues that can potentially interact with VEGF and that differ between VEGFR1 and VEGFR2 are labeled. Yellow and blue: VEGF. Green: VEGFR1 D2. White: VEGFR1 D3. Analysis points to a more extensive interaction between VEGF and VEGFR1 D3 compared to VEGFR2 D3.

Fig S1

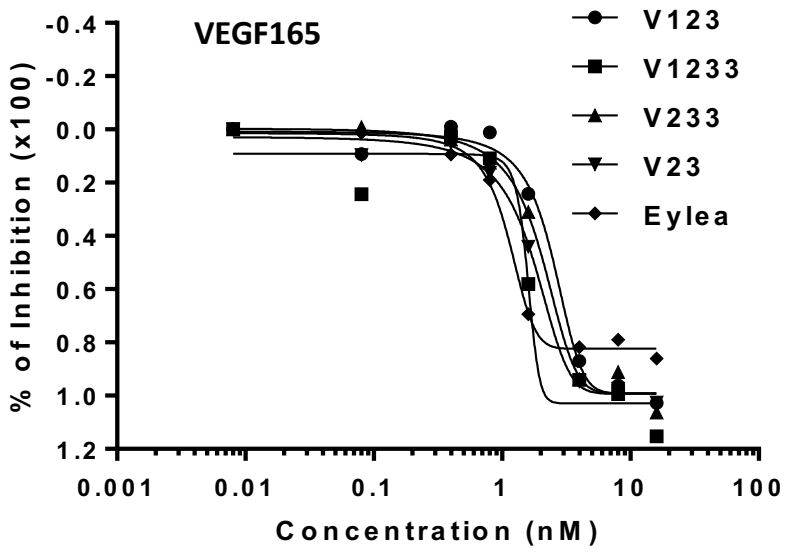
VEGF165
V123
V1233
V233
V23
Eylea
% of Inhibition (x100)
-0.4
-0.2
0.0
0.2
0.4
0.6
0.8
1.0
1.2
0.001
0.01
0.1
1
10
100
Concentration (nM)

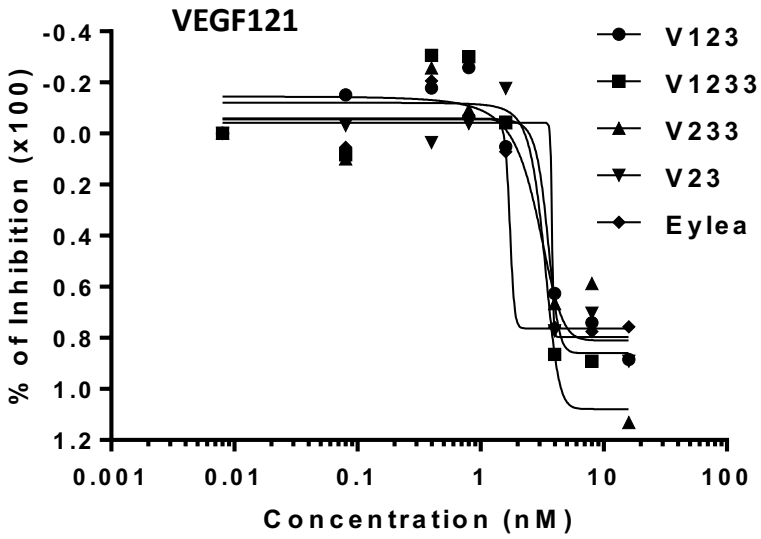
VEGF121
V123
V1233
V233
V23
Eylea
% of Inhibition (x100)
-0.4
-0.2
0.0
0.2
0.4
0.6
0.8
1.0
1.2
0.001
0.01
0.1
1
10
100
Concentration (nM)

Fig. S2

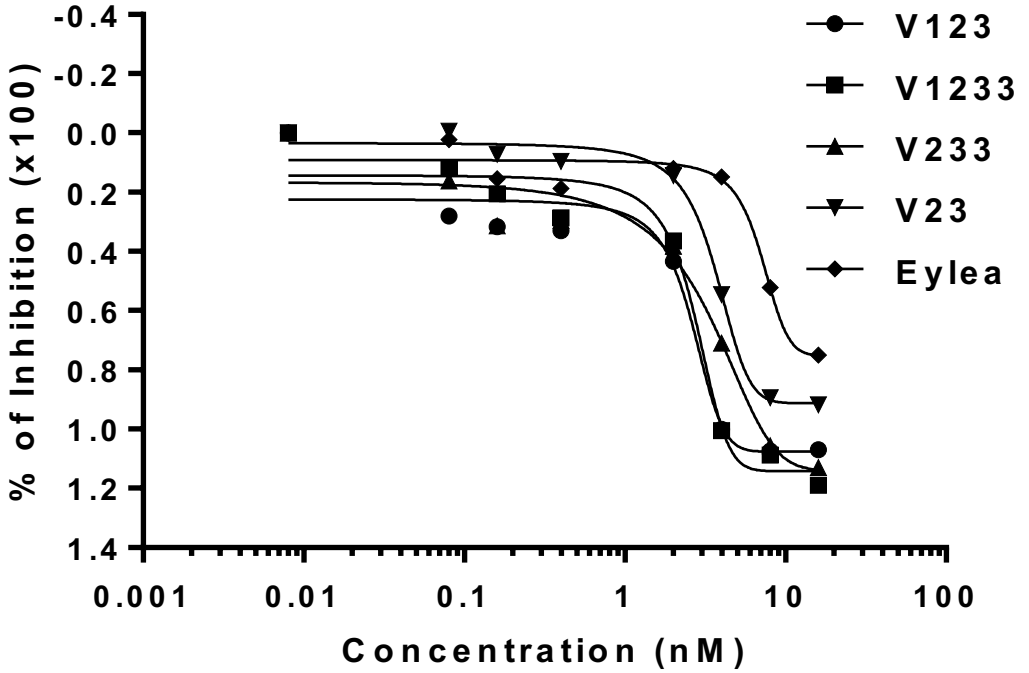
-0.4
-0.2
0.0
0.2
0.4
0.6
0.8
1.0
1.2
1.4
% of Inhibition (x100)
0.001
0.01
0.1
1
10
100
Concentration (nM)
V123
V1233
V233
V23
Eylea

Fig S3

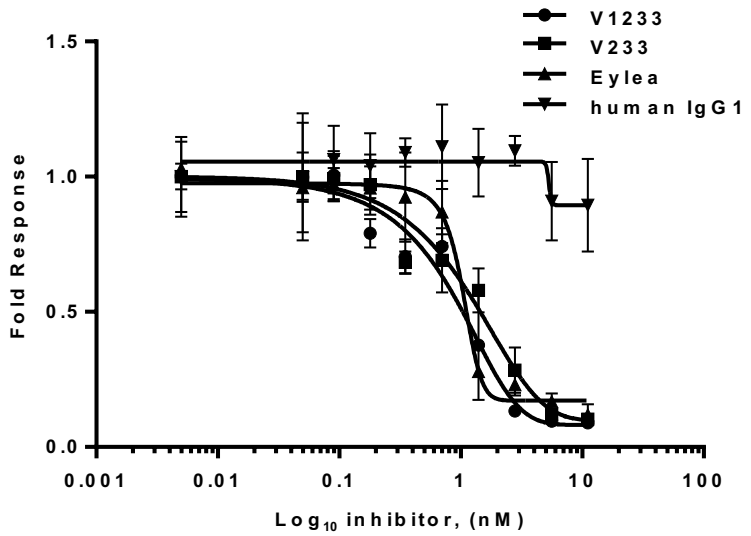
V1233
V233
Eylea
human IgG1
1.5
1.0
0.5
0.0
Fold Response
0.001
0.01
0.1
1
10
100
Log10 inhibitor, (nM)

Fig S4

References

1. V. Lambert *et al*., Laser-induced choroidal neovascularization model to study age-related macular degeneration in mice. *Nat Protoc* **8**, 2197-2211 (2013).
2. R. L. E. Silva *et al*., Tyrosine kinase blocking collagen IV-derived peptide suppresses ocular neovascularization and vascular leakage. *Sci Transl Med* **9** (2017).
3. L. E. Smith *et al*., Essential role of growth hormone in ischemia-induced retinal neovascularization. *Science* **276**, 1706-1709 (1997).
4. J. Chen, K. M. Connor, C. M. Aderman, L. E. Smith, Erythropoietin deficiency decreases vascular stability in mice. *J Clin Invest* **118**, 526-533 (2008).
5. T. A. Gardiner *et al*., Inhibition of tumor necrosis factor-alpha improves physiological angiogenesis and reduces pathological neovascularization in ischemic retinopathy. *Am J Pathol* **166**, 637-644 (2005).
6. J. Chen *et al*., Suppression of retinal neovascularization by erythropoietin siRNA in a mouse model of proliferative retinopathy. *Invest Ophthalmol Vis Sci* **50**, 1329-1335 (2009).
7. L. P. Aiello *et al*., Suppression of retinal neovascularization in vivo by inhibition of vascular endothelial growth factor (VEGF) using soluble VEGF-receptor chimeric proteins. *Proc Natl Acad Sci USA* **92**, 10457-10461 (1995).
8. S. Xiao *et al*., Fully automated, deep learning segmentation of oxygen-induced retinopathy images. *JCI Insight* **21, e97585** (2017).